

Minute SiGe Quantum Dots on Si(001) by a Kinetic 3D Island Mode

R. Koch,¹ G. Wedler,² J.J. Schulz,^{1,2} and B. Wassermann²

¹Paul-Drude-Institut für Festkörperelektronik, Hausvogteiplatz 5-7, D-10117 Berlin, Germany

²Institut für Experimentalphysik, Freie Universität Berlin, Arnimallee 14, D-14195 Berlin, Germany

(Received 14 December 2000; published 11 September 2001)

We investigated the initial growth stages of $\text{Si}_x\text{Ge}_{1-x}/\text{Si}(001)$ by real time stress measurements and *in situ* scanning tunneling microscopy at deposition temperatures, where intermixing effects are still minute (≤ 900 K). Whereas $\text{Ge}/\text{Si}(001)$ is a well known Stranski-Krastanow system, the growth of SiGe alloy films switches to a 3D island mode at Si content above 20%. The obtained islands are small (a few nanometers), are uniform in shape, and exhibit a narrow size distribution, making them promising candidates for future quantum dot devices.

DOI: 10.1103/PhysRevLett.87.136104

PACS numbers: 68.55.Ac, 68.35.Gy, 68.37.Ef, 81.15.-z

A key parameter for the evolution of film morphology with film thickness is the growth mode. In recent years the Stranski-Krastanow (SK) mode of IV-IV [1,2] and III-V [3,4] semiconductor systems has attracted strong attention offering the prospect of fabricating uniform quantum dot arrays for electronics and solid state laser devices. The strain field of these heteroepitaxial SK systems favors the formation of regularly shaped self-assembled nanostructures with a narrow size distribution, which, however, is still too broad for a technological application.

In this context the growth of Ge or SiGe alloy films on Si(001) has served as an intensively studied model system. In the case of $\text{Ge}/\text{Si}(001)$ the transition from 2D to 3D growth takes place at thicknesses of 3–5 monolayers (ML) depending on the deposition temperature [5]. After passing a prepyramid roughening stage [6] small dislocation-free elongated pyramids (“huts”) appear [1], which on further growth are substituted by more rounded larger islands (“domes”) [7,8]. Real time stress measurements revealed that part of the ideal misfit strain of about 4% is already relieved in the Ge wetting layer [5], which exhibits a network of dimer row vacancies and dimer vacancy lines [6,7]. Further strain relief takes place when the 3D islanding sets in [5,9,10], in accordance with theoretical predictions [11–13]. The growth of $\text{Si}_x\text{Ge}_{1-x}$ alloy films has been found to be qualitatively identical to $\text{Ge}/\text{Si}(001)$ [14]. However, as concluded from the stress evolution as well as *ex situ* AFM (atomic force microscopy) and transmission electron microscopy, the wetting layer thickness of the lower misfit strain films is significantly increased, e.g., to 38 ML (≈ 5 nm) for $\text{Si}_{0.8}\text{Ge}_{0.2}$ deposited at 900 K [15].

Here we report on real time intrinsic stress measurements (ISM) combined with *in situ* STM (scanning tunneling microscope) investigation of $\text{Si}_x\text{Ge}_{1-x}/\text{Si}(001)$ which focus on the initial growth stages. All films were deposited at 900 K or lower in order to minimize intermixing effects. Recent studies revealed considerable intermixing at 970–1020 K [16], typical growth temperatures for SiGe films. For instance, upon Ge deposition at 1020 K the effective quantum dot volume was found to be about 4 times

higher than the amount of deposited Ge because of enormous Si in-diffusion [17]. At 900 K, on the other hand, intermixing is of minor importance [18]. In contrast to previous work, our study discloses a change of the underlying growth mechanism. At Si concentrations above 20% the growth mode switches from SK to a kinetic 3D island mode, where no wetting layer is formed. The obtained 3D islands are small (a few nm), are uniform in shape, and exhibit a narrow size distribution. Therefore the new growth mode discovered in the SiGe system provides a promising alternative path for the fabrication of SiGe quantum dots.

The experiments were performed in an interconnected multiple chamber UHV system (base pressure $< 10^{-10}$ hPa) equipped with a sensitive cantilever beam (CB) device for *in situ* stress measurements [19], a four-grid LEED (low energy electron diffraction) optics for *in situ* control of the substrate and film quality, as well as a homebuilt UHV-STM for *in situ* structural investigations. In each experimental run a CB and an STM substrate were prepared simultaneously. After carefully outgassing the substrate holder at 900 K for many hours, the oxide was desorbed by heating to 1300 K until eventually sharp (1×2) LEED spots were obtained. Then the substrates were slowly cooled down to the deposition temperature and thermally equilibrated for 1 h. Ge was evaporated from a Knudsen-type boron nitride crucible; Si was electron beam evaporated from a rod of undoped Si. The deposition rates of both sources were controlled individually by two calibrated quartz crystal microbalances and adjusted so that the total rate was 0.008 ± 0.002 nm/s. The pressure during deposition was better than 3×10^{-9} hPa. Immediately after film preparation the STM sample was transferred to the STM chamber without breaking UHV and imaged at room temperature. In addition, thicker films were investigated by AFM after exposure to air. For comparison a number of experiments was performed on direct current heated substrates (see below).

The stress behavior of $\text{Si}_x\text{Ge}_{1-x}/\text{Si}(001)$ in the broad concentration range of $0 \leq x \leq 0.8$ is illustrated in Fig. 1. The respective film forces, plotted as a function of the

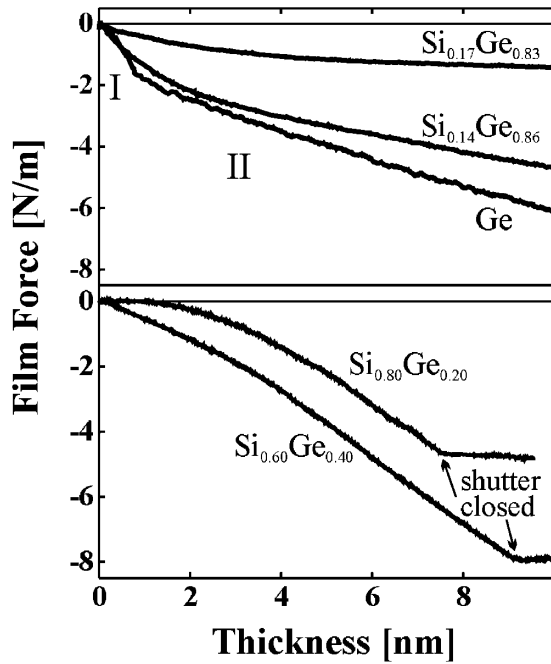


FIG. 1. Film forces (i.e., integral forces in films of unit width) measured in real time during the deposition of various $\text{Si}_x\text{Ge}_{1-x}$ films onto Si(001) at 900 K.

average $\text{Si}_x\text{Ge}_{1-x}$ thickness in Fig. 1, were measured in real time during deposition. To facilitate comparison we also included the force curve of pure Ge from Ref. [5]. By the term “film force” we denote the total force F acting in a film of unit width [N/m] (i.e., analogous to the definition of surface stress). The average stress is obtained as usual by dividing the normalized force by the film thickness. Accordingly, the slope of the force curves corresponds to the instantaneous film stress.

Comparison of the upper and lower diagrams of Fig. 1 reveals that the stress evolution of $\text{Si}_x\text{Ge}_{1-x}/\text{Si}(001)$ is highly sensitive to the Si content. At low Si concentrations (<20%) the shape of the force curves is consistent with the SK mode. As discussed in detail in Ref. [5] a steep increase of compressive force is observed initially, i.e., during growth of the wetting layer (*stress regime I* in [5]); when the 3D islanding sets in, the film forces increase with a smaller slope due to the partial strain relief in isolated clusters (*stress regime II* in [5]). In the case of pure Ge the wetting layer is about 0.8 nm thick (≈ 5.5 ML); its stress of 2.6 GPa ($\sigma_{\text{exp}}^{\text{I}}$ in Table I) is only half of the theoretical misfit stress at 900 K (5.2 GPa) due to partial strain relief by dimer and dimer row vacancies (see discussion above). The 3D islanding reduces the instantaneous stress further to 0.9 GPa ($\sigma_{\text{exp}}^{\text{II}}$ in Table I) corresponding to a total strain relief of more than 80%. Up to Si concentrations of 14%, the stress behavior remains qualitatively the same. Quantitatively, the wetting layer stress at 14% is slightly reduced to 2.0 GPa, and the wetting layer thickness has increased to 1.3 nm. It is noteworthy that the latter value compares well with the critical layer thickness of 1.1 nm predicted by

TABLE I. Theoretical misfit strain ϵ_0 of various $\text{Si}_x\text{Ge}_{1-x}/\text{Si}(001)$ films at 900 K and corresponding misfit stress σ_0 calculated by Hooke’s law; the biaxial modulus E_{biax} of the alloy films was estimated via Vegard’s rule from the moduli of pure Ge and Si at 900 K. $\sigma_{\text{exp}}^{\text{I}}$ and $\sigma_{\text{exp}}^{\text{II}}$ are the experimental stress values of stress regimes I and II, respectively (see text).

$\text{Si}_x\text{Ge}_{1-x}$	ϵ_0 ^{900 K}	$E_{\text{biax}}^{\text{900 K}}$ (GPa)	$\sigma_0^{\text{900 K}}$ (GPa)	$\sigma_{\text{exp}}^{\text{I}}$ (GPa)	$\sigma_{\text{exp}}^{\text{II}}$ (GPa)
Ge	0.042	123	5.2	2.6	0.9
$\text{Si}_{0.14}\text{Ge}_{0.86}$	0.036	129	4.6	2.0	0.3
$\text{Si}_{0.17}\text{Ge}_{0.83}$	0.035	130	4.5	0.8	0.2
$\text{Si}_{0.58}\text{Ge}_{0.42}$	0.018	148	2.7	0.7	1.1
$\text{Si}_{0.80}\text{Ge}_{0.20}$	0.009	158	1.3	~ 0	1.1
Si	0	167	0	0	...

theory for dislocation insertion into $\text{Si}_{0.14}\text{Ge}_{0.86}$ films [20]. Surprisingly, a further slight increase of the Si concentration to 17% leads to a nearly complete disappearance of stress. While $\sigma_{\text{exp}}^{\text{I}}$ has decreased to 0.8 GPa corresponding to a strain relief of more than 85%, no further strain is transmitted in regime II.

At Si concentrations above 20% a fundamental change in the stress behavior is observed. The stress in regime I is very small with values of $\sigma_{\text{exp}}^{\text{I}} < 0.8$ GPa. In regime II, on the other hand, the stress increases assuming values that are significantly larger than $\sigma_{\text{exp}}^{\text{I}}$; for instance, $\sigma_{\text{exp}}^{\text{II}}$ of the $\text{Si}_{0.80}\text{Ge}_{0.20}$ film matches almost the theoretical misfit stress of 1.3 GPa. Note that the average stress of thicker SiGe films even exceeds the stress of high misfit Ge/Si(001). Particularly the latter finding, i.e., $\sigma_{\text{exp}}^{\text{II}}$ exceeding $\sigma_{\text{exp}}^{\text{I}}$, is indeed astonishing and in clear contradiction to a SK mode. According to theory [11–13] the 2D/3D transition of SK mode proceeds in order to reduce elastic energy; it is therefore necessarily accompanied by strain relief and thus a decrease of the instantaneous stress (i.e., $\sigma_{\text{exp}}^{\text{II}} < \sigma_{\text{exp}}^{\text{I}}$).

Further insight is provided by our *in situ* STM investigations of the $\text{Si}_{0.60}\text{Ge}_{0.40}$ and $\text{Si}_{0.80}\text{Ge}_{0.20}$ films. The large scale top views of Fig. 2 reveal that both films consist of 3D islands even at the low mean thickness of 1 nm. The

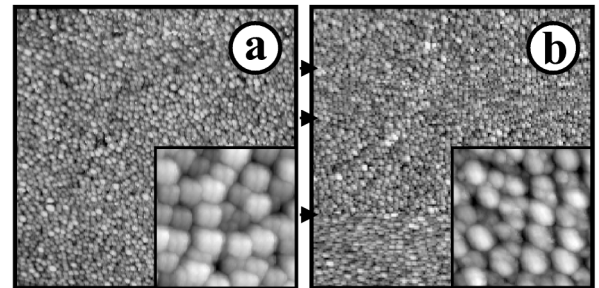


FIG. 2. $250 \times 250 \text{ nm}^2$ STM top view of 1 nm thick films of (a) $\text{Si}_{0.60}\text{Ge}_{0.40}$ and (b) $\text{Si}_{0.80}\text{Ge}_{0.20}$; in (b) subsequent terraces of the substrate can be recognized (marked by arrows). Insets show areas of $32 \times 32 \text{ nm}^2$.

average island diameter is about 5 nm; the island height ranges from 1.5 to 2.5 nm. The total island volume determined from the STM images yields a mean film thickness of 1.3 ± 0.4 nm. Because of tip convolution effects, which are enhanced by narrow island separation, the STM certainly overestimates the island volume. Nevertheless, our *in situ* STM results clearly point to a wetting layer well below 1 nm, exhibiting a maximum thickness of 1–2 ML. A possible wetting layer therefore is orders of magnitude thinner than the critical layers for misfit dislocations of $\text{Si}_{0.60}\text{Ge}_{0.40}$ and $\text{Si}_{0.80}\text{Ge}_{0.20}$ films with thicknesses of 11 and 110 nm, respectively [20], and even thinner than that of pure Ge films. In conjunction with the stress results the structural information obtained by STM provides strong evidence that the growth mode of SiGe films changes from SK mode to a 3D island mode at higher Si contents. The absence of a wetting layer explains the low stress values observed in regime I, where the immediate nucleation of 3D islands is responsible for an efficient relief of the misfit strain. Both films of Fig. 2 are already close to percolation, which takes place at thicknesses not higher than 2–3 nm. When the 3D islands merge, most of the misfit strain is recovered; obviously the island size at percolation is too small to favor insertion of misfit dislocations (ideal separation for $\epsilon_0 = 1\%$: ≈ 40 nm). *In situ* STM and *ex situ* AFM investigations of thicker films (not shown here) exhibit the typical morphology of postpercolation films, characterized by a broad continuous layer with a root mean square roughness of 2–3 nm.

Finally, it is worth discussing the size distribution of the SiGe islands in more detail. Statistical analysis of the STM images reveals an average island diameter of 5.5 ± 0.94 nm and 4.6 ± 0.86 nm, respectively (Fig. 3), which is about 2 orders of magnitude smaller than the quantum dots obtained at 1030 K [21]. The island size distribution is very narrow both compared with islands obtained by the thermodynamic Volmer-Weber mode [22] and also with regard to Ge/Si(001), where the coexistence of elongated huts and domes gives rise to a double-peaked size distribution [23]. Postdeposition annealing as well as variation of the film thickness may further improve island uniformity.

How can we understand this unexpected switch of the growth mode, which at first sight even seems to be contradictory to previous studies? The main difference to previous work certainly is the procedure of the substrate preparation. Commonly the Si(001)(1 × 2) surface is prepared by direct current heating with the oxide being removed by a short flash to 1500–1600 K. The cantilever beam substrates of the present study (and for comparison also the free-standing STM substrates) were radiatively heated from the backside to about 1300 K—a temperature regime where carbide formation is critical. In order to rule out carbon contaminations to affect nucleation [24] we performed a series of supplementary STM investigations on direct current heated samples. Figure 4a shows a conventionally prepared Si(001) surface that is characterized by

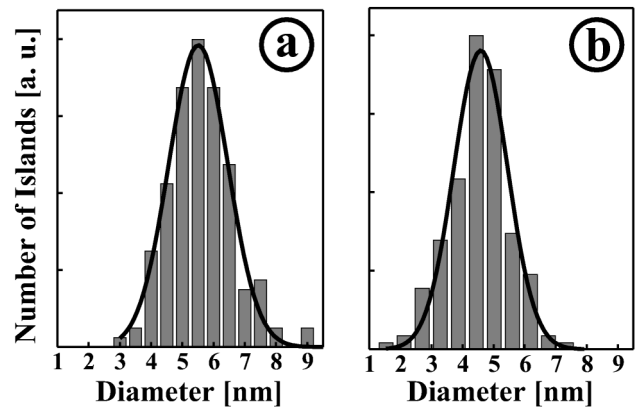


FIG. 3. Size distribution of the 1 nm thick films of (a) $\text{Si}_{0.60}\text{Ge}_{0.40}$ and (b) $\text{Si}_{0.80}\text{Ge}_{0.20}$; the superimposed solid lines are Gaussian fits.

extended nearly perfectly (1 × 2) reconstructed terraces (Fig. 4b). After deposition of 1 nm $\text{Si}_{0.70}\text{Ge}_{0.30}$ at 900 K (Fig. 4c) the surface still exhibits extended flat terraces patterned by (2 × n) trenches analogous to pure Ge films [7], thus pointing to film growth proceeding by the SK mode. For substrate preparation at lower temperatures we started from chemically etched, Shiraki-type Si(001) substrates to avoid carbon contamination. On the substrates used here (known as SPM samples) thin passivating oxide layer is prepared by a final etching treatment in a solution of $\text{H}_2\text{SO}_4/\text{H}_2\text{O}_2$ (4:1, 90 °C, 10 min) [25] yielding oxygen desorption temperatures of only 900–1000 K. Figures 4d and 4e show a sample heated for 1 h at 970 K at a pressure of $(2-3) \times 10^{-10}$ hPa. Compared to the only few missing

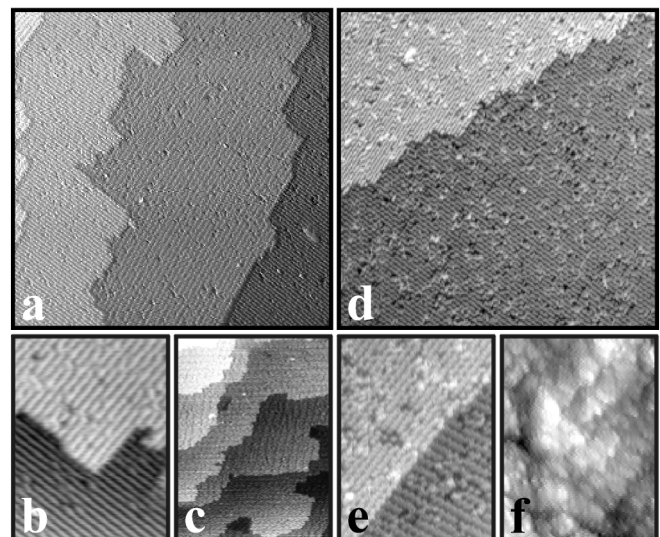


FIG. 4. (a) $60 \times 60 \text{ nm}^2$ STM top view of a conventionally prepared Si(001) sample; (b) higher magnification image; (c) $73 \times 96 \text{ nm}^2$ top view after deposition of 1 nm $\text{Si}_{0.70}\text{Ge}_{0.30}$. (d) $60 \times 60 \text{ nm}^2$ STM top view of a Shiraki-type Si(001) sample (see text); (e) higher magnification image; (f) $33 \times 44 \text{ nm}^2$ top view after deposition of 1 nm $\text{Si}_{0.70}\text{Ge}_{0.30}$.

or adsorbed dimers observed typically on conventionally prepared substrates (e.g., Fig. 4b) the surface of the SPM substrate exhibits a high density of intrinsic defects; extended aggregates of missing dimers and single ad-dimers trapped in their neighborhood as well as $c(2 \times 4)$ dimer stacking are observed frequently. We remark that upon shorter heating for oxide removal (as used in Ref. [25]) the defect density is further increased with even larger dimer vacancies. A short flash to 1500 K of the SPM samples, on the other hand, leads to well ordered terraces similar to Fig. 4a [26]. Figure 4f shows the SPM sample after deposition of 1 nm Si_{0.70}Ge_{0.30} at 900 K. In contrast to Fig. 4c a corrugated film morphology typical of island growth is observed, thus demonstrating that immediate nucleation of 3D islands is favored on the defect-rich surfaces. Nucleation obviously takes place at the larger dimer vacancies of the Si(001) surface suggesting that the island density can be controlled by the dimer vacancy concentration. Therefore the final island size may be optimized by varying the procedure of substrate preparation.

In conclusion, by employing two powerful *in situ* methods, ISM and STM, to study the early growth stages of SiGe alloy films on Si(001), we discovered that the growth mode switches from SK mode to a kinetic 3D island mode at Si contents above 20%, when the substrate surface contains extended dimer vacancies as intrinsic defects. Despite the lower misfit of SiGe compared to pure Ge the islands are very small (~ 5 nm) and uniformly shaped and sized, thus making them promising candidates for future quantum dot devices.

We thank K.-H. Rieder for his continuous support, G. Behme and J. Schönberg for the AFM investigations, and Mrs. L. Perepelittchenko for preparation of the SPM substrates. The work was sponsored by the Deutsche Forschungsgemeinschaft (Ko-1313, Sfb 296).

-
- [1] Y.-W. Mo, D. E. Savage, B. S. Swartzentruber, and M. G. Lagally, Phys. Rev. Lett. **65**, 1020 (1990).
 - [2] D. J. Eaglesham and M. Cerullo, Phys. Rev. Lett. **64**, 1943 (1990).
 - [3] S. Guha, A. Madhukar, and K. C. Rajkumar, Appl. Phys. Lett. **57**, 2110 (1990).
 - [4] A. Kurtenbach, K. Eberl, and T. Shitara, Appl. Phys. Lett. **66**, 361 (1995).

- [5] G. Wedler, J. Walz, T. Hesjedal, E. Chilla, and R. Koch, Phys. Rev. Lett. **80**, 2382 (1998).
- [6] A. Vailionis, B. Cho, G. Glass, P. Desjardins, D. G. Cahill, and J. E. Greene, Phys. Rev. Lett. **85**, 3672 (2000).
- [7] M. Tomitori, K. Watanabe, M. Kobayashi, and O. Nishikawa, Appl. Surf. Sci. **76/77**, 322 (1994).
- [8] G. Medeiros-Ribeiro, A. M. Bratkovski, T. I. Kamins, D. A. A. Ohlberg, and R. S. Williams, Science **279**, 353 (1998).
- [9] A. J. Schell-Sorokin and R. M. Tromp, Phys. Rev. Lett. **64**, 1039 (1990).
- [10] A. J. Steinfort, P. M. L. O. Scholte, A. Ettema, F. Tuinstra, M. Nielsen, E. Landemark, D.-M. Smilgies, R. Feidenhans'l, G. Falkenberg, L. Seehofer, and R. L. Johnson, Phys. Rev. Lett. **77**, 2009 (1996).
- [11] J. Tersoff and R. M. Tromp, Phys. Rev. Lett. **70**, 2782 (1993).
- [12] V. A. Shchukin, N. N. Ledentsov, P. S. Kop'ev, and D. Bimberg, Phys. Rev. Lett. **75**, 2968 (1995).
- [13] E. Pehlke, N. Moll, A. Kley, and M. Scheffler, Appl. Phys. A **65**, 525 (1997).
- [14] J. A. Floro, E. Chason, R. D. Twesten, R. Q. Hwang, and L. B. Freund, Phys. Rev. Lett. **79**, 3946 (1997).
- [15] J. A. Floro, E. Chason, L. B. Freund, R. D. Twesten, R. Q. Hwang, and G. A. Lucadamo, Phys. Rev. B **59**, 1990 (1999).
- [16] J. Walz, T. Hesjedal, E. Chilla, and R. Koch, Appl. Phys. A **69**, 467 (1999).
- [17] G. Wedler, J. Walz, T. Hesjedal, E. Chilla, and R. Koch, Appl. Phys. A **69**, 467 (1999).
- [18] R. Koch, B. Wassermann, and G. Wedler, *Defect and Diffusion Forum* (Scitec Publications Ltd., Ütikon-Zürich, Switzerland, 2000), Vols. 183–185, p. 95.
- [19] M. Weber, R. Koch, and K. H. Rieder, Phys. Rev. Lett. **73**, 1166 (1994).
- [20] R. People and J. C. Bean, Appl. Phys. Lett. **47**, 322 (1985).
- [21] J. A. Floro, G. A. Lucadamo, E. Chason, L. B. Freund, M. Sinclair, R. D. Twesten, and R. Q. Hwang, Phys. Rev. Lett. **80**, 4717 (1998).
- [22] H. Jaeger, P. D. Mercer, and R. G. Sherwood, Surf. Sci. **11**, 265 (1968).
- [23] L. Vescan, M. Goryll, T. Stoica, P. Gartner, K. Grimm, O. Chretien, E. Mateeva, C. Dieker, and B. Holländer, Appl. Phys. A **71**, 423 (2000).
- [24] O. G. Schmidt, C. Lange, K. Eberl, O. Kienzle, and F. Ernst, Appl. Phys. Lett. **71**, 2340 (1997).
- [25] H. Okumura, T. Akane, Y. Tsubo, and S. Matsumoto, J. Electrochem. Soc. **144**, 3765 (1997).
- [26] J. J. Schulz, B. Wassermann, G. Wedler, and R. Koch (to be published).